INSTITUT DE FRANCE
Académie des sciences

Comptes Rendus
Mécanique

Sara Chikhi, Mohammed Debiane and Nabil Allalou

On the sub-harmonic instabilities of three-dimensional interfacial gravity–capillary waves in infinite depths

Volume 350 (2022), p. 191-203

Published online: 12 May 2022

https://doi.org/10.5802/crmeca.111

Les Comptes Rendus. Mécanique *sont membres du Centre Mersenne pour l'édition scientifique ouverte*
www.centre-mersenne.org
e-ISSN : 1873-7234

Comptes Rendus
Mécanique
2022, 350, p. 191-203
https://doi.org/10.5802/crmeca.111

Short paper / *Note*

On the sub-harmonic instabilities of three-dimensional interfacial gravity–capillary waves in infinite depths

Sara Chikhi *, [a], **Mohammed Debiane** [a] **and Nabil Allalou** [a]

[a] Université des Sciences et de la Technologie Houari Boumediene, Faculté de Physique, BP 32 El Alia, Alger 1611, Algérie

E-mails: scusthb@gmail.com (S. Chikhi), debianemd@yahoo.fr (M. Debiane), n_allalou2004@yahoo.fr (N. Allalou)

Abstract. In order to analyze the stability of gravity–capillary short-crested waves propagating at the interface of two fluids of infinite depths, a numerical procedure has been developed using a collocation method. The three-dimensional wave is generated by an oblique reflection of a uniform wave train arriving at a vertical wall at some angle of incidence θ measured from the perpendicular to the wall. Fixing the reflection at angle $\theta = 45°$, and wave steepness at $h = 0.25$, we studied the influence of the density ratio μ and the inverse Bond number δ on the unstable area and the growth rate. It was observed that the unstable regions and the maximum growth rate decrease when μ and δ increase. Also, we found that the dominant instability belongs to the Class Ib as in the case of free-surface gravity waves in deep water.

Keywords. Linear stability, Sub-harmonic perturbation, Three-dimensional waves, Gravity–capillary waves, Interfacial waves, Short-crested water waves.

Manuscript received 10th October 2021, revised 19th April 2022, accepted 21st April 2022.

1. Introduction

The problem of the linear instabilities of three-dimensional short-crested water waves was investigated in several works. Iouallalen *et al.* [1] studied numerically the linear stability of three-dimensional progressive gravity waves, proving that the two-dimensional progressive waves are more unstable than the three-dimensional progressive waves. Also it was found that the dominant instabilities are sub-harmonic in the direction of propagation of the basic wave for small wave steepness in the range $0 \leq h \leq 0.30$. Iouallalen *et al.* [1] show that the timescales of harmonic resonances corresponding to these sub-harmonic resonances are smaller than those given by Iouallalen *et al.* [2]. To study the linear stability of symmetric short-crested water waves,

* Corresponding author.

Badulin *et al.* [3] used two complementary basic techniques that led to the analysis of an eigenvalue problem. The first approach, developed by Iouallalen *et al.* [1, 2], is achieved through the application of the Galerkin method to a set of linearized Euler equations; the second is based on the Zakharov's [4] Hamiltonian formulation for water waves. Comparison with asymptotic results in the small-amplitude limit has verified the capacity of the methods used in Iouallalen *et al.* [1, 2] to present the whole picture of instabilities, including the smallest details of weak "bubble" instabilities. Iouallalen *et al.* [5] have studied the three regimes of instability for three-dimensional surface gravity waves propagating on water of finite depth. They found that the geometry of the perturbed wave fields are more complex than those in deep water. They have also shown that the depth parameter has a critical restabilization value beyond which the timescales of surface wave variation shorten exponentially. The wave steepness and degree of three-dimensionality of the unperturbed wave field determine this critical value. Using the numerical procedure developed by Iouallalen *et al.* [1], Kimoun *et al.* [6] have investigated the impact of the wave steepness on the instability of short-crested gravity waves in deep water. They found that these waves are unstable to Class I modulation perturbation near to the two-dimensional standing waves limit and to Class II near to the two-dimensional progressive waves limit, while the fully three-dimensional waves match the two limits. Iouallalen *et al.* [7] computed numerically the complete set of solutions of a short-crested wave. They found that the structure of the solutions is composed of three branches and a turning point that matches two of them. By computing the stability of the bifurcating solutions along their branches they discovered another bubble of instability close to the turning point of the solutions. Also they noted a bubble of instability associated with resonance interactions, and another super-harmonic instability close to the bifurcation point. Allalou *et al.* [8] have investigated numerically the super-harmonic instability of interfacial gravity short-crested waves subjected to infinitesimal perturbations. Focusing on the (2, 6) harmonic, they found that the most unstable case associated with these harmonic resonance was for $\mu = 0.08$, also that the interfacial waves are quasi-stable for a density ratio around $\mu = 0.34$ while for $0 \leq \mu \leq 1$ the size of instability bubbles is weak.

The aim of the present study is to extend the work of Iouallalen *et al.* [1] and Allalou *et al.* [8] to study the linear stability of three-dimensional waves propagating at the interface of two fluids of infinite depths.

2. Mathematical modeling

The fluids are supposed to be homogeneous, incompressible and inviscid, and the motion is assumed to be irrotational. The physical variables associated with the lower fluid are denoted by a superscript (2) and those of the upper fluid by a superscript (1). A Cartesian coordinate system (x, y, z) is adopted with the x- and y-axes located on the still-water plane and the z-axis pointing vertically upward. The variables and the equations will be written in dimensionless form with reference length $1/k$, reference time $1/\sqrt{gk}$ and reference density ρ_2. g is the gravitational acceleration, and k the wavenumber of the incident wave train. To compute short-crested waves, it is helpful to use the frame of reference (X, Y, Z), where

$$X = \alpha x - \omega t, \quad Y = \beta y, \quad Z = z$$

and in which the short-crested wave is steady with period 2π in X and Y. Here ω is the non-dimensional frequency and p and q are the non-dimensional wavenumbers in the X and Y directions, respectively, defined by

$$\alpha = \sin\theta \quad \text{and} \quad \beta = \cos\theta.$$

The set of equations governing irrotational gravity–capillary waves on the interface of two layers of inviscid and incompressible fluids having infinite depths is

$$p^2\Phi_{1,XX} + q^2\Phi_{1,YY} + \Phi_{1,ZZ} = 0 \qquad \eta < Z < +\infty \tag{1}$$

$$p^2\Phi_{2,XX} + q^2\Phi_{2,YY} + \Phi_{2,ZZ} = 0 \qquad -\infty < Z < \eta \tag{2}$$

$$-\omega\eta_X + p^2\Phi_{1,X}\eta_X + q^2\Phi_{1,Y}\eta_Y - \Phi_{1,Z} = 0 \qquad \text{on } Z = \eta \tag{3}$$

$$-\omega\eta_X + p^2\Phi_{2,X}\eta_X + q^2\Phi_{2,Y}\eta_Y - \Phi_{2,Z} = 0 \qquad \text{on } Z = \eta \tag{4}$$

$$\begin{aligned} &-\frac{\mu}{1-\mu}\left(-\omega\Phi_{1,X} + \frac{1}{2}\left(p^2\Phi_{1,X}^2 + q^2\Phi_{1,Y}^2 + \Phi_{1,Z}^2 +\right)^2\right) \\ &\quad + \frac{1}{1-\mu}\left(-\omega\Phi_{2,X}\frac{1}{2}\left(p^2\Phi_{2,X}^2 + q^2\Phi_{2,Y}^2 + \Phi_{2,Z}^2\right)^2\right) + \eta \qquad \text{on } Z = \eta \\ &\quad - \delta\xi(X,Y) = 0 \end{aligned} \tag{5}$$

$$\Phi_{1z} = 0 \qquad \text{for } z \to +\infty \tag{6}$$

$$\Phi_{2z} = 0 \qquad \text{for } z \to -\infty \tag{7}$$

with

$$\xi(X,Y) = \frac{\eta_{XX}(1+\eta_Y^2) + \eta_{YY}(1+\eta_X^2) - 2\eta_{XY}\eta_X\eta_Y}{(1+\eta_X^2+\eta_Y^2)^{3/2}} \tag{8}$$

$$\delta = \frac{Tk^2}{g(\rho_2 - \rho_1)}.$$

And where $\Phi_1(X,Y,Z)$ and $\Phi_2(X,Y,Z)$ are the velocity potentials of the upper and lower fluids respectively, $Z = \eta((X,Y))$ is the interface equation, $\mu = \rho_1/\rho_2$ is the density ratio, and T is the surface tension.

The system of equations (1)–(8) admit steady doubly periodic solutions:

$$\eta(X,Y) = \sum_{i=1}\sum_{mn} A_{mn}^{(i)}\cos(mX)\cos(mY)h^{(i)} \tag{9}$$

$$\Phi_1(X,Y,Z) = \sum_{i=1}\sum_{mn} B_{mn}^{(i)}\sin(mX)\cos(mY)\exp(-\gamma_{mn})h^{(i)} \tag{10}$$

$$\Phi_2(X,Y,Z) = \sum_{i=1}\sum_{mn} C_{mn}^{(i)}\sin(mX)\cos(mY)\exp(\gamma_{mn})h^{(i)} \tag{11}$$

$$\omega = \sum_{i=0}\omega_i h^{(i)}, \tag{12}$$

where $\gamma_{mn} = \sqrt{(m^2\alpha^2 + n^2\beta^2)}$. The perturbation parameter h is the wave steepness defined as

$$h = \tfrac{1}{2}\left(\overline{\eta}(0.0) - \overline{\eta}(\pi\cdot 0)\right).$$

To construct the stability problem, let us define a frame of reference $\mathscr{R}^*(x^*,y^*,z^*)$ with $x^* = x - Ct$, $y^* = y$, $z^* = z$, $t^* = t$ and $\Phi^* = \Phi - Cx^*$. C is the propagation velocity of the interfacial wave. The system of equations (1)–(8) is then reformulated in terms of the new variables.

The stability problem consists in assuming that the surface elevation and the velocity potentials are a superposition of a steady unperturbed wave $(\overline{\eta}, \overline{\Phi_1}, \overline{\Phi_2})$ and small unsteady harmonic perturbations $(\eta', \Phi_1', \Phi_2')$, that is to say

$$\eta(x,y,t) = \overline{\eta}(x,y) + \eta'(x,y,t) \tag{13}$$

$$\Phi_1(x,y,z,t) = \overline{\Phi_1}(x,y,z) + \Phi_1'(x,y,z,t) \tag{14}$$

$$\Phi_2(x,y,z,t) = \overline{\Phi_2}(x,y,z) + \Phi_2'(x,y,z,t), \tag{15}$$

where $\Phi_1' \ll \overline{\Phi_1}, \Phi_2' \ll \overline{\Phi_2}, \eta' \ll \overline{\eta}$. Expressions (13)–(15) are substituted into the new system of equations which is then linearized. The first order of equations, which represents the stability problem, is then

$$\Phi'_{1,xx} + \Phi'_{1,yy} + \Phi'_{1,zz} = 0 \qquad \text{for } \overline{\eta}(x,y) < z < +\infty \tag{16}$$

$$\Phi'_{2,xx} + \Phi'_{2,yy} + \Phi'_{2,zz} = 0 \qquad \text{for } -\infty < z < \overline{\eta}(x,y) \tag{17}$$

$$\begin{aligned}\eta'_t &+ (\overline{\Phi}_{1,x}\eta'_x + \Phi'_{1,x}\overline{\eta}_x) + (\overline{\Phi}_{1,y}\eta'_y + \Phi'_{1,y}\overline{\eta}_y)\\ &+ \eta'(\overline{\eta}_x\overline{\Phi}_{1,xz} + \overline{\eta}_y\overline{\Phi}_{1,yz} - \overline{\Phi}_{1,zz}) - \Phi'_{1,z} = 0 \qquad \text{on } z = \overline{\eta}(x,y)\end{aligned} \tag{18}$$

$$\begin{aligned}\eta'_t &+ (\overline{\Phi}_{2,x}\eta'_x + \Phi'_{2,x}\overline{\eta}_x) + (\overline{\Phi}_{2,y}\eta'_y + \Phi'_{2,y}\overline{\eta}_y)\\ &+ \eta'(\overline{\eta}_x\overline{\Phi}_{2,xz} + \overline{\eta}_y\overline{\Phi}_{2,yz} - \overline{\Phi}_{2,zz}) - \Phi'_{2,z} = 0 \qquad \text{on } z = \overline{\eta}(x,y)\end{aligned} \tag{19}$$

$$\begin{aligned}&\frac{1}{1-\mu}\Big[\Phi'_{2,t} + \Phi'_{2,x}\overline{\Phi}_{2,x} + \Phi'_{2,y}\overline{\Phi}_{2,y} + \Phi'_{2,z}\overline{\Phi}_{2,z}\\ &\quad + \eta'(\overline{\Phi}_{2,x}\overline{\Phi}_{2,xz} + \overline{\Phi}_{2,y}\overline{\Phi}_{2,yz} + \overline{\Phi}_{2,z}\overline{\Phi}_{2,zz})\Big]\\ &- \frac{\mu}{1-\mu}\Big[\Phi'_{1,t} + \Phi'_{1,x}\overline{\Phi}_{1,x} + \Phi'_{1,y}\overline{\Phi}_{1,y} + \Phi'_{1,z}\overline{\Phi}_{1,z} \qquad \text{on } z = \overline{\eta}(x,y)\\ &\quad + \eta'(\overline{\Phi}_{1,x}\overline{\Phi}_{1,xz} + \overline{\Phi}_{1,y}\overline{\Phi}_{1,yz} + \overline{\Phi}_{1,z}\overline{\Phi}_{1,zz})\Big] + \eta'\\ &- \delta\xi^{(1)}(x,y) = 0\end{aligned} \tag{20}$$

$$\Phi'_{1,z} = 0 \qquad \text{for } z \to +\infty \tag{21}$$

$$\Phi'_{2,z} = 0 \qquad \text{for } z \to -\infty, \tag{22}$$

where

$$\begin{aligned}\xi^{(1)}(x,y) = &\left\{\left(\frac{2\overline{\eta}_{xx}\overline{\eta}_y - 2\overline{\eta}_{xy}\overline{\eta}_x}{(1+\overline{\eta}_x^2+\overline{\eta}_y^2)^{3/2}} - 3\frac{\overline{\eta}_y\overline{\eta}_{xx}(1+\overline{\eta}_y^2) + \overline{\eta}_y\overline{\eta}_{yy}(1+\overline{\eta}_x^2) - 2\overline{\eta}_y^2\overline{\eta}_x\overline{\eta}_{xy}}{(1+\overline{\eta}_x^2+\overline{\eta}_y^2)^{5/2}}\right)\eta'_y\right.\\ &+\left(\frac{2\overline{\eta}_{yy}\overline{\eta}_x - 2\overline{\eta}_{xy}\overline{\eta}_y}{(1+\overline{\eta}_x^2+\overline{\eta}_y^2)^{3/2}} - 3\frac{\overline{\eta}_x\overline{\eta}_{xx}(1+\overline{\eta}_y^2) + \overline{\eta}_x\overline{\eta}_{yy}(1+\overline{\eta}_x^2) - 2\overline{\eta}_x^2\overline{\eta}_y\overline{\eta}_{xy}}{(1+\overline{\eta}_x^2+\overline{\eta}_y^2)^{5/2}}\right)\eta'_x\\ &+\left(\frac{(1+\overline{\eta}_y^2)}{(1+\overline{\eta}_x^2+\overline{\eta}_y^2)^{3/2}}\right)\eta'_{xx} + \left(\frac{(1+\overline{\eta}_x^2)}{(1+\overline{\eta}_x^2+\overline{\eta}_y^2)^{3/2}}\right)\eta'_{yy} + \left(\frac{-2\overline{\eta}_y\overline{\eta}_x}{(1+\overline{\eta}_x^2+\overline{\eta}_y^2)^{3/2}}\right)\eta'_{xy}\Big\}.\end{aligned} \tag{23}$$

We look for non-trivial solutions of the following form:

$$\begin{pmatrix}\eta'\\ \Phi'_1\\ \Phi'_2\end{pmatrix} = \mathrm{e}^{-\mathrm{i}\sigma t}\mathrm{e}^{\mathrm{i}(px+qy)}\begin{pmatrix}\displaystyle\sum_{J=-\infty}^{J=+\infty}\sum_{K=-\infty}^{K=+\infty} a_{JK}\mathrm{e}^{\mathrm{i}(J\alpha x+K\beta y)}\\ \displaystyle\sum_{J=-\infty}^{J=+\infty}\sum_{K=-\infty}^{K=+\infty} b_{JK}\mathrm{e}^{\mathrm{i}(J\alpha x+K\beta y)}\mathrm{e}^{-\kappa_{JK}z}\\ \displaystyle\sum_{J=-\infty}^{J=+\infty}\sum_{K=-\infty}^{K=+\infty} c_{JK}\mathrm{e}^{\mathrm{i}(J\alpha x+K\beta y)}\mathrm{e}^{\kappa_{JK}z}\end{pmatrix}, \tag{24}$$

where

$$\kappa_{JK} = \sqrt{[(p+J\alpha)^2 + (q+K\beta)^2]}.$$

In the linear stability problem, we seek to determine the set of eigenvalues σ and the components a_{JK}, b_{jk}, c_{jk} of their associated eigenvectors.

3. Linear instability condition

Since the system of equations (16)–(23) is real valued, the eigenvalues appear in complex conjugate pairs. Thus instability corresponds to $\mathrm{Im}(\sigma) \neq 0$. For $h = 0$ the unperturbed wave is given by $\overline{\eta} = 0$, $\overline{\Phi_1} = -C_0 x$ and $\overline{\Phi_2} = -C_0 x$, with $C_0 = \omega_0/\alpha$. The eigenvalues are:

$$\sigma^s_{JK} = s\left(\frac{1-\mu}{1+\mu}\right)^{1/2} \sqrt{\gamma_{JK}}(1+\delta((p+J\alpha)^2+(q+K\beta)^2))^{1/2} - C_0(p+J\alpha),$$

with $s = \mp 1$ and $\omega_0 = \sqrt{((1+\delta)(1-\mu))/(1+\mu)}$.

The wave is neutrally stable for $h = 0$ due to the real-valued set of the eigenvalues. As the wave steepness h rises, instabilities can emerge. As Iouallalen *et al.* [1] did, we apply the required condition for instability to Hamiltonian systems in terms of collision of eigenvalues of opposite signatures s or at zero frequency: nonlinear effects ($h > 0$) can lead to instability if two modes have the same frequency, that is $\sigma^s_{J_1K_1} = \sigma^{-s}_{J_2K_2}$. The loss of stability can be expressed by:

$$\begin{aligned}&((p+\alpha J_1)^2+(q+\beta K_1)^2)^{1/4} \times (1+\delta((p+\alpha J_1)^2+(q+\beta K_1)^2))^{1/2}\\ &\quad+((p+\alpha J_2)^2+(q+\beta K_2)^2)^{1/4}\\ &\quad\times(1+\delta((p+\alpha J_2)^2+(q+\beta K_2)^2))^{1/2} = (J_1-J_2)\times\sqrt{1+\delta}.\end{aligned} \tag{25}$$

The coalescence of two eigenvalues may be interpreted as a resonance caused by the interaction between two infinitesimal modes of wave vectors $\vec{k}_1$ and $\vec{k}_2$ and the basic wave with fundamental eigenvectors $\vec{k}_{01}$ and $\vec{k}_{02}$. According to Phillips *et al.* [9], the interactions can only exist if the following conditions are simultaneously satisfied.

$$\vec{k}_1 + \vec{k}_2 = \sum_i \mp\vec{k}_{0i} \quad \omega'_1 \mp \omega'_2 = \sum_i \mp\omega'_{0i}.$$

Here, ω'_1, ω'_2 and ω'_{0i} are the frequencies of the disturbances and the unperturbed wave in a fixed frame of reference respectively. Following Iouallalen *et al.* [1], the solutions of (25) are classified in two classes according to the parity of the integer $(J_1 - J_2)$: Class I and Class II correspond respectively to even and odd $(J_1 - J_2)$. This lets us to choose J_1 and J_2 such that

$$\begin{aligned}&J_1 = j \text{ and } J_2 = -j && \text{for the Class I } (j)\\ &J_1 = j \text{ and } J_2 = -j-1 && \text{for the Class II } (j).\end{aligned}$$

In this investigation, we focus on the Class I, and Class II, for $j = 1$ corresponding to dominant resonances. Owing to the triangular symmetry of a short-crested wave, m and n are integers of the same parity for the harmonic (m, n). For any instability, mixed-parity eigenmodes require mixed-parity modes of the unperturbed wave. Therefore, no instability appears for mixed-parity eigenmodes. Thus, instability requires K_1 and K_2 satisfy

$$\begin{aligned}&K_1 = \pm 1 \text{ and } K_2 = \pm 1 && \text{for the Class I}\\ &K_1 = \pm 1 \text{ and } K_2 = \pm 1 && \text{for the Class II.}\end{aligned}$$

For each class, two subclasses can be defined, depending on the interacting modes. Classes Ia and Ib correspond to the interaction of four waves and Classes IIa and IIb correspond to the interaction of five waves. We obtain the same classes as Iouallalen *et al.* [1] complemented by the capillary.

3.1. *Class Ia* ($j = 1, K_1 = K_2 = 1$) *or Class Ia′* ($j = 1, K_1 = K_2 = -1$)

For Class Ia of instabilities, Equation (25) can be written in the following form

$$\begin{aligned}&((p+\alpha)^2+(q+\beta)^2)^{1/4}(1+\delta((p+\alpha)^2+(q+\beta)^2))^{1/2}\\ &\quad+((p-\alpha)^2+(q+\beta)^2)^{1/4}(1+\delta((p-\alpha)^2+(q+\beta)^2))^{1/2}\\ &\quad=2\sqrt{1+\delta}.\end{aligned} \tag{26}$$

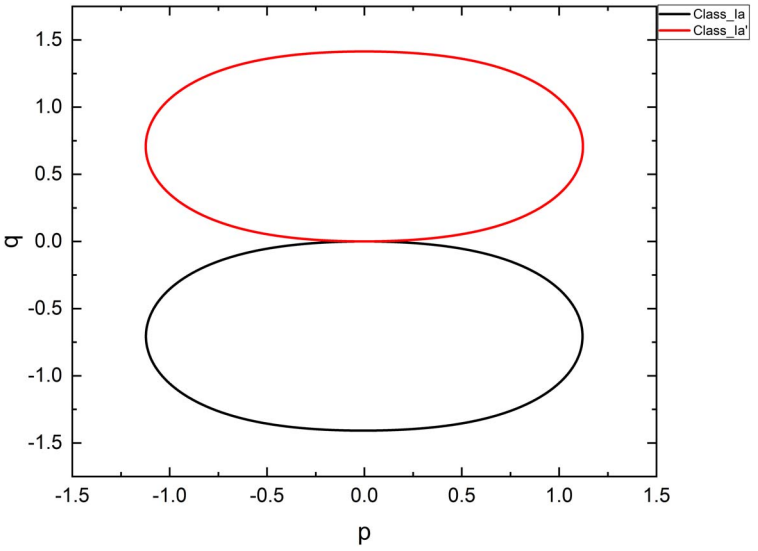

Figure 1. Resonance curves of Class Ia and Class Ia′ for $\delta = 0.002$, and $\theta = 45°$.

The resonance curves corresponding to Class Ia and Class Ia′ for the angle considered hereafter are plotted in Figure 1.

This stability diagram corresponds to the following resonance:

$$\vec{k}_1 = \vec{k}_2 + \vec{k}_{01} + \vec{k}_{02}$$
$$\omega_1' = \omega_2' + 2\omega_0'.$$

Here,

$$\vec{k}_1 = (p+\alpha, q+\beta)^t, \quad \vec{k}_2 = (p-\alpha, q+\beta)^t, \quad \vec{k}_{01} = (\alpha, \beta)^t, \quad \vec{k}_{02} = (\alpha, -\beta)^t$$
$$\omega_1' = \sqrt{|\vec{k}_1|}(1+\delta((p+\alpha)^2+(q+\beta)^2))^{1/2}, \quad \omega_1' = -\sqrt{|\vec{k}_1|}(1+\delta((p-\alpha)^2+(q+\beta)^2))^{1/2},$$
$$\omega_0' = \sqrt{1+\delta}.$$

3.2. *Class Ib* ($j = 1, K_1 = 1, K_2 = -1$) *or Class Ib′* ($j = 1, K_1 = -1, K_2 = -1$)

For the Class Ib, Equation (25) becomes:

$$((p+\alpha)^2+(q+\beta)^2)^{1/4}(1+\delta((p+\alpha)^2+(q+\beta)^2))^{1/2} + ((p-\alpha)^2+(q-\beta)^2)^{1/4}(1+\delta((p-\alpha)^2+(q-\beta)^2))^{1/2} = 2\sqrt{1+\delta}. \tag{27}$$

Resonance curves corresponding to Class Ib and Class Ib′ are plotted in Figure 2.

The phenomenon of resonance corresponds to

$$\vec{k}_1 = \vec{k}_2 + 2\vec{k}_{01}$$
$$\omega_1' = \omega_2' + 2\omega_0',$$

with

$$\vec{k}_1 = (p+\alpha, q+\beta)^t, \quad \vec{k}_2 = (p-\alpha, q-\beta)^t, \quad \vec{k}_{01} = (\alpha, \beta)^t$$
$$\omega_1' = \sqrt{|\vec{k}_1|}(1+\delta((p+\alpha)^2+(q+\beta)^2))^{1/2}, \quad \omega_2' = -\sqrt{|\vec{k}_1|}(1+\delta((p-\alpha)^2+(q-\beta)^2))^{1/2},$$
$$\omega_0' = \sqrt{1+\delta}.$$

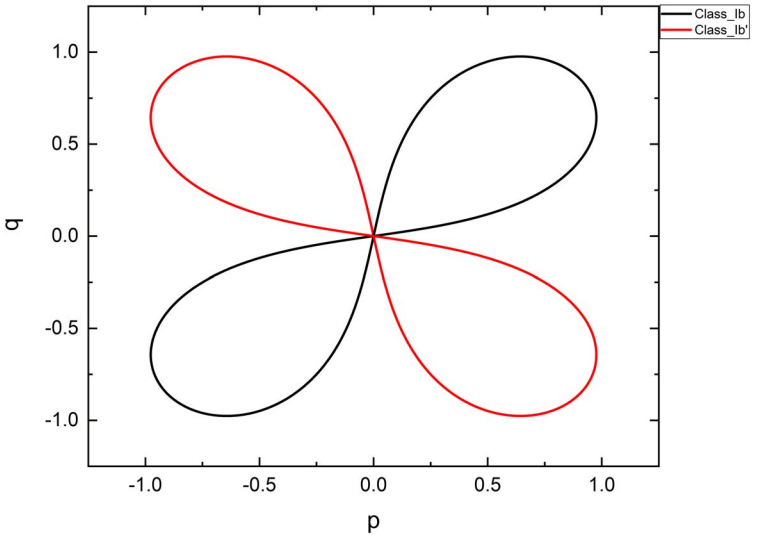

Figure 2. Resonance curves of both Class Ib and Class Ib$'$ for $\delta = 0.002$, and $\theta = 45°$.

3.3. *Class IIa* ($j = 1, K_1 = 1, K_2 = 2$) *or Class IId*$'$ $j = 1, K_1 = -1, K_2 = -2$)

For Class IIa, the resonance condition (25) becomes:

$$\begin{aligned}&((p+\alpha)^2+(q+\beta)^2)^{1/4}(1+\delta((p+\alpha)^2+(q+\beta)^2))^{1/2}\\&\quad+((p-2\alpha)^2+(q+2\beta)^2)^{1/4}(1+\delta((p-2\alpha)^2+(q+2\beta)^2))^{1/2}\\&=3\times\sqrt{1+\delta}.\end{aligned}\tag{28}$$

Resonance curves corresponding to Class Ib and Class Ib$'$ are displayed in Figure 3. The resonance conditions become:

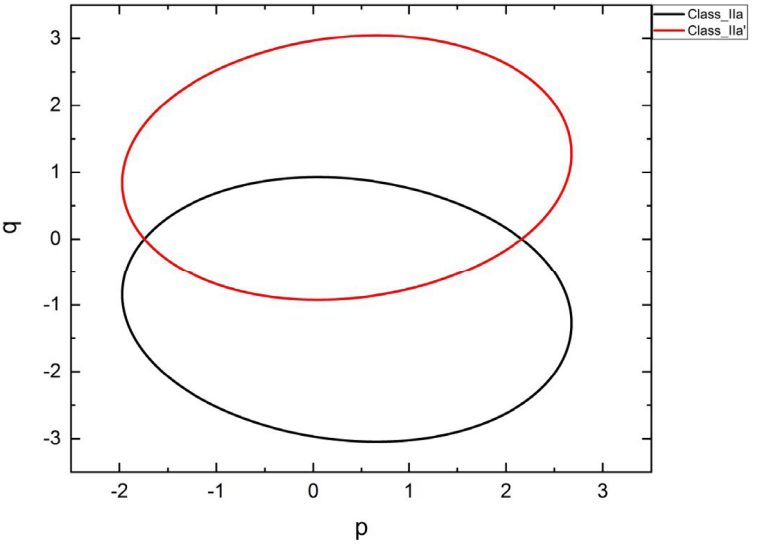

Figure 3. Resonance curves of both Class IIa and Class IIa$'$, for $\delta = 0.002$ and $\theta = 45°$.

$$\vec{k}_1 = \vec{k}_2 + \vec{k}_{01} + 2\vec{k}_{02}$$
$$\omega'_1 = \omega'_2 + 3\omega'_0$$

with

$$\vec{k}_1 = (p+\alpha, q+\beta)^t, \quad \vec{k}_2 = (p-2\alpha, q+2\beta)^t, \quad \vec{k}_{01} = (\alpha,\beta)^t, \quad \vec{k}_{02} = (\alpha,-\beta)^t$$
$$\omega'_1 = \sqrt{|\vec{k}_1|}(1+\delta((p+\alpha)^2+(q+\beta)^2))^{1/2}, \quad \omega'_2 = -\sqrt{|\vec{k}_1|}(1+\delta((p-2\alpha)^2+(q+2\beta)^2))^{1/2},$$
$$\omega'_0 = \sqrt{1+\delta}.$$

3.4. *Class IIb* ($j=1, K_1=1, K_2=-2$) *or Class IIb′* ($j=1, K_1=-1, K_2=2$)

For Class IIb, Equation (25) may be written in the form:

$$\begin{aligned}&((p+\alpha)^2+(q+\beta)^2)^{1/4}(1+\delta((p+\alpha)^2+(q+\beta)^2))^{1/2}\\ &\quad+((p-2\alpha)^2+(q-2\beta)^2)^{1/4}(1+\delta((p-2\alpha)^2+(q-2\beta)^2))^{1/2}\\ &=3\sqrt{1+\delta}.\end{aligned} \tag{29}$$

Resonance curves corresponding to Class IIb and Class IIb′ are shown in Figure 4. The resonance conditions become:

$$\vec{k}_1 = \vec{k}_2 + 3\vec{k}_{01}$$
$$\omega'_1 = \omega'_2 + 3\omega'_0,$$

with

$$\vec{k}_1 = (p+\alpha, q+\beta)^t, \quad \vec{k}_2 = (p-2\alpha, q-2\beta)^t, \quad \vec{k}_{01} = (\alpha,\beta)^t$$
$$\omega'_1 = \sqrt{|\vec{k}_1|}(1+\delta((p+\alpha)^2+(q+\beta)^2))^{1/2}, \quad \omega'_2 = -\sqrt{|\vec{k}_1|}(1+\delta((p-2\alpha)^2+(q-2\beta)^2))^{1/2},$$
$$\omega'_0 = \sqrt{1+\delta}.$$

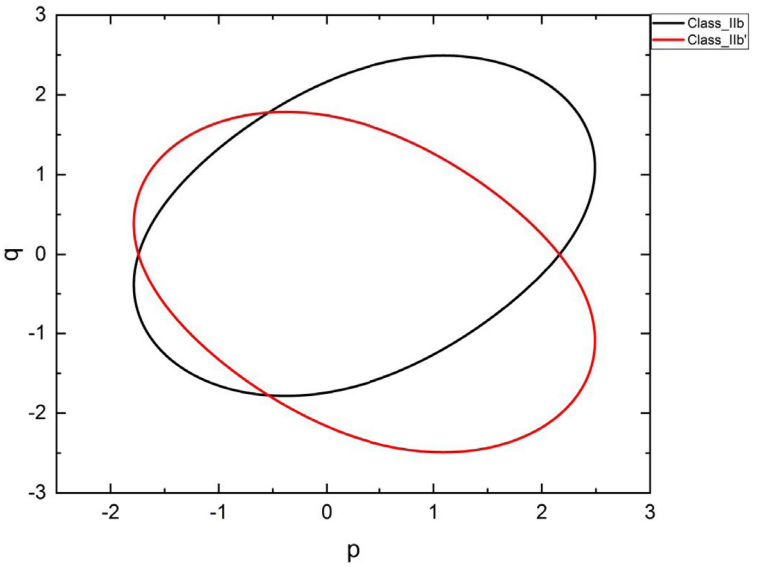

Figure 4. Resonance curves of both Class IIb and Class IIb′, for $\delta = 0.002$, and $\theta = 45°$.

4. Numerical results

A validation of our numerical code was carried out for $\kappa = 0$, $\mu = 0.1$, $\theta = 10°$ and $h = 0.15$. Table 1 represents a comparison of the maximum amplification rates calculated by our numerical code with the results obtained by Allalou *et al.* [8]. The table shows that the values of amplification rates are very close, with a slight difference related to the method used to find the maximum.

Table 1. Comparison between computed values of the maximum amplification rates with the present method and those given by Allalou *et al.* [8], $\mu = 0.1$, $\theta = 10°$ $h = 0.15$

h	Present method	Allalou *et al.*
	Class_Ia	
	$0.30877832 \times 10^{-2}$	$0.31447499 \times 10^{-2}$
	Class_Ib	
0.15	$0.17499196 \times 10^{-2}$	$0.17533445 \times 10^{-2}$
	Class_IIa	
	$4.68316181 \times 10^{-4}$	5.1894626×10^{-4}
	Class_IIb	
	$4.24942437 \times 10^{-5}$	3.0740997×10^{-5}

For fixed values of wave steepness $h = 0.25$, and angle $\theta = 45°$, we have generated the instability regions for two values of surface tension parameter, $\delta = 0.001$ and $\delta = 0.002$. This value of θ, which is neither too large nor too small corresponds to fully three-dimensional short-crested waves. The instabilities are detected by exploring the area around the linear resonance curves in the (p, q) plane. For each case, the impact of the fluid stratification on the stability of interfacial gravity–capillary waves was investigated using different values of density ratio $\mu = \{0.1, 0.3, 0.5, 0.7, 0.9\}$.

For $\delta = 0.001$, the instability regions of Class Ia and Ib are plotted in Figure 5, for $\mu = 0.1$, and Figure 6, for $\mu = 0.5$. Similar plots are shown in Figures 7 and 8 for $\delta = 0.002$.

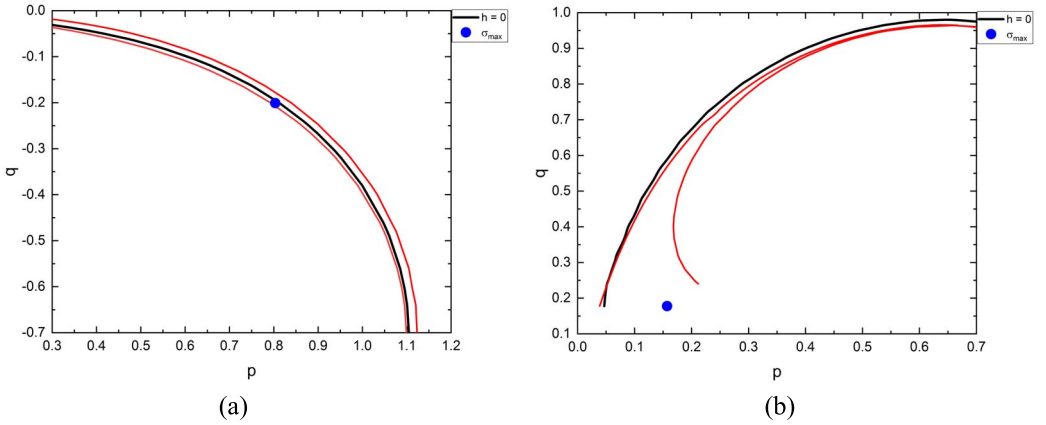

Figure 5. Instability regions for $\theta = 45°$, $h = 0.25$, $\delta = 0.001$ and $\mu = 0.1$. The labelled dots correspond to the maximum growth rate of the instability. (a) Class Ia, (b) Class Ib.

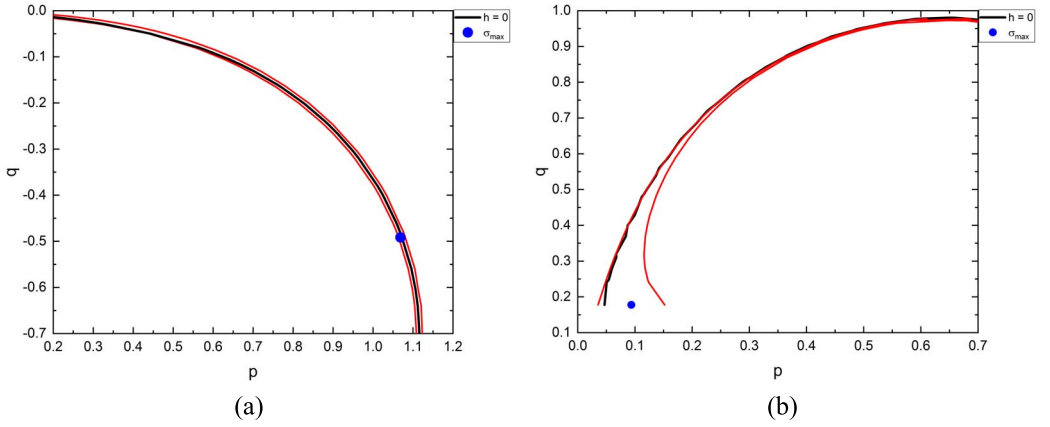

Figure 6. Instability regions for $\theta = 45°$, $h = 0.25$, $\delta = 0.001$ and $\mu = 0.5$. The labelled dots correspond to the maximum growth rate of the instability. (a) Class Ia, (b) Class Ib.

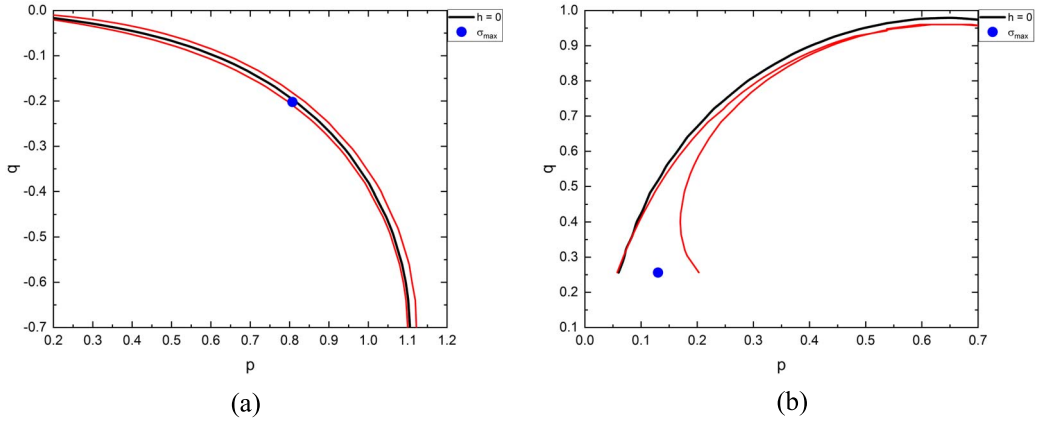

Figure 7. Instability regions for $\theta = 45°$, $h = 0.25$, $\delta = 0.002$ and $\mu = 0.1$. The labelled dots correspond to the maximum growth rate of the instability. (a) Class Ia, (b) Class Ib.

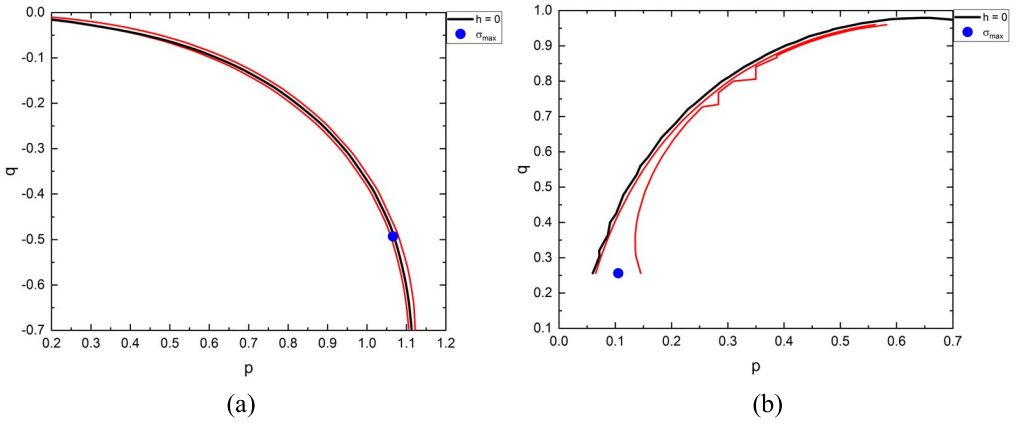

Figure 8. Instability regions for $\theta = 45°$, $h = 0.25$, $\delta = 0.002$ and $\mu = 0.5$. The labelled dots correspond to the maximum growth rate of the instability. (a) Class Ia, (b) Class Ib.

It can be noted that, for a fixed value of the inverse Bond number δ, the unstable region shrunk when the density ratio was increased. Thus, if we decrease the density ratio, a degree of stability is introduced. Similarly, for a fixed value of μ, the unstable region expanded when the interfacial tension was decreased. This is due to the stabilizing effect of the surface tension. Since the stabilizing effect of surface tension is more effective the shorter the wave, its presence is expected to make the instabilities of longer waves more important. From these examples, we remark that the unstable disturbances of both Classes Ia, and Ib are sub-harmonic in the two orthogonal horizontal directions.

The maximum growth rates of all classes considered here are plotted in Figure 9 as a function of the density ratio μ, for two values of the inverse Bond number: (a) $\delta = 0.001$, and (b) $\delta = 0.002$. Overall it is shown that the maximum growth rate decreases as μ increases. These results show that, for this angle representative of fully three-dimensional short-crested waves, Class Ib instabilities are dominant as in the case of free-surface gravity waves in deep water.

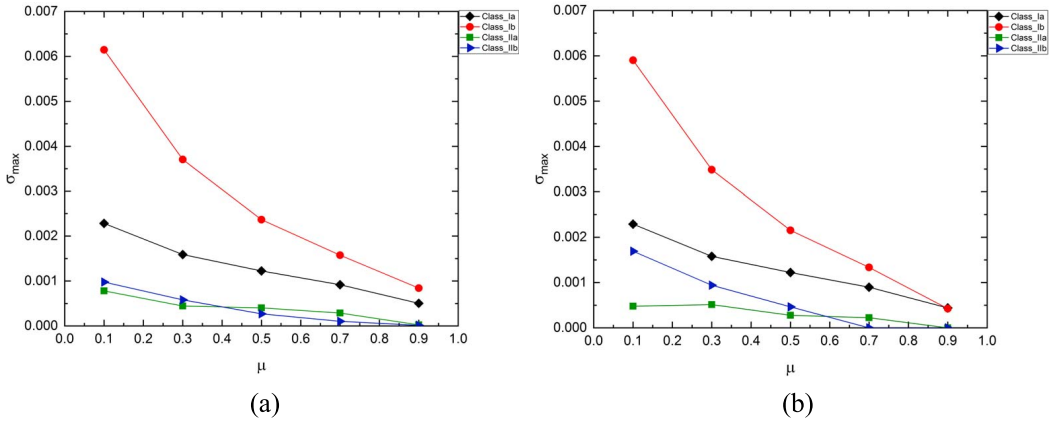

Figure 9. Maximum growth rates of Class I and Class II, as a function of the density ratio μ. (a) $\delta = 0.001$, (b) $\delta = 0.002$.

The second effect on the maximum growth rate to consider is that produced by the surface tension. In most practical situations, the effect of the density ratio occurs together with the effect of surface tension, but it is important to differentiate them in the analysis to understand their individual influence. To do this, we have grouped, in each of Figures 10a, b, c, d, the curves concerning each class, for $\delta = 0.001$ and $\delta = 0.002$. For Classes Ia and Ib the curves corresponding to $\delta = 0.002$ are located below those corresponding to $\delta = 0.001$, indicating the stabilizing effect of the surface tension. This is clearer for large values of μ. For Classes IIa and IIb, this effect is clearly observed only for large values of μ. We can observe that Class 1Ia instabilities disappear from $\mu \approx 0.9$ for $\delta = 0.001$ and $\delta = 0.002$. Class IIb instabilities disappear from $\mu \approx 0.9$ for $\delta = 0.001$ and from $\mu \approx 0.7$ for $\delta = 0.002$.

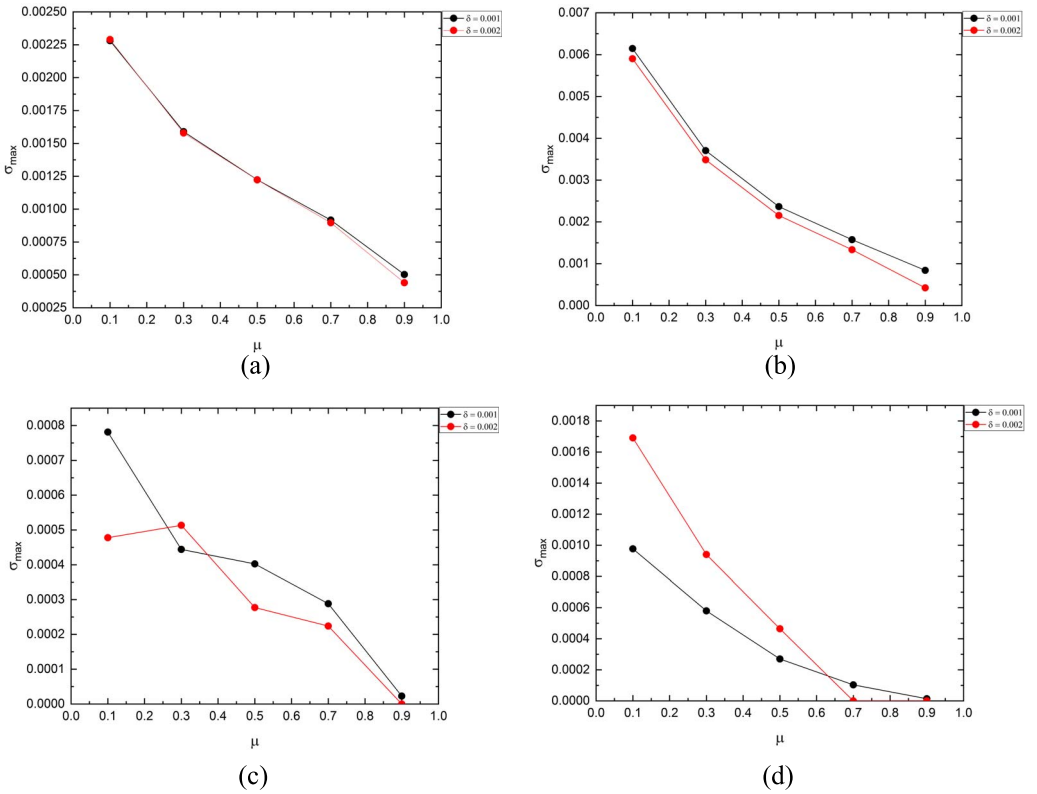

Figure 10. Maximum growth rates for $\delta = 0.001$ (graph in black) and $\delta = 0.002$ (graph in red) as a function of the density ratio μ. (a) Class Ia, (b) Class Ib, (c) Class IIa, (d) Class IIb.

5. Conclusion

A numerical procedure based on the collocation method has been developed to investigate the stability of gravity–capillary short-crested waves propagating at the interface of two fluids of infinite depths. We examined the effect of the density ratio and the inverse Bond number on the unstable area and the maximum growth rate of a fully developped short-crested wave of wave steepness $h = 0.25$. It was observed that the unstable regions and the maximum growth rate decrease when μ and δ increase. Also, we found that the dominant instability belongs to the Class Ib as in the case of free-surface gravity waves in deep water.

However, the maximum growth rates of all of the classes decrease rapidly as μ increases, to disappear at a density ratio $\mu = 0.9$ for Class IIa, and Class IIb of the case $\delta = 0.001$, and at $\mu = 0.7$ for the same two classes of the second case of capillary. Also for the two cases, the dominant instability belongs to Class Ib.

Conflicts of interest

Authors have no conflict of interest to declare.

Acknowledgements

The authors would like to warmly thank M. Iouallalen and K. Kharif for providing the code they developed for the collocation method in the case of free-surface short-crested gravity waves.

References

[1] M. Iouallalen, C. Kharif, "On the subharmonic instabilities of steady three-dimensional deep water waves", *J. Fluid Mech.* **262** (1994), p. 265-291.
[2] M. Iouallalen, C. Kharif, "Fourth order approximation of short-crested waves", *C. R. Acad. Sci. Paris* **316** (1993), p. 1193-1200.
[3] S. Badulin, I. Shrira, C. Kharif, M. Iouallalen, "On two approaches to the problem of instability of short-crested water waves", *J. Fluid Mech.* **303** (1995), p. 297-326.
[4] V. E. Zakharov, "Stability of periodic waves of finite amplitude on the surface of a deep, fluid", *J. Appl. Mech. Tech. Phys. (USSR)* **2** (1968), p. 190-194.
[5] M. Iouallalen, C. Kharif, A. J. Roberts, "Stability regimes of finite depth short-crested water waves", *J. Phys. Oceanogr.* **29** (1999), p. 2318-2331.
[6] O. Kimmoun, M. Iouallalen, C. Kharif, "Instabilities of steep short-crested surface waves in deep water", *Phys. Fluids* **11** (1999), p. 1679-1681.
[7] M. Iouallalen, M. Okamura, "Structure of the Instability associated with harmonic resonance of short-crested waves", *J. Phys. Oceanogr.* **32** (2002), p. 1331-1337.
[8] N. Allalou, M. Debiane, C. Kharif, "On the superharmonic instability of nonlinear three-dimensional interfacial waves of two infinite layers", *Eur. J. Mech. B Fluids* **59** (2016), p. 135-139.
[9] O. M. Phillips, "On the dynamics of unsteady gravity waves of finite amplitude", *J. Fluid Mech.* **9** (1960), p. 193-217.